J. Webster (ed.), *Wiley Encyclopedia of Electrical and Electronics Engineering*

PHASED ARRAY ANTENNAS

A receiving antenna is a spatial sampler of the incident electric field. It provides an estimate of the incident field by performing a spatial averaging or integration of the impinging electric fields along the physical length of the antenna. The purpose of a complex antenna element or an antenna array is to carry out spatial filtering, that is, to select the incident fields arriving from some preferred directions or having some spatiotemporal properties and to zero out the response along other directions. Two of the most prevalent applications of spatial filtering are radio direction finding and adaptive processing.

In radio direction finding the objective is to estimate the angle of arrival and intensities of the various signals by measuring a set of induced voltages in the elements of an antenna array. So from the given physical dimensions and geometry of the array and the measured noise-contaminated voltages induced in the antenna elements, the goal is to estimate both the directions of arrival and strengths of the various signals. In Fig. 1 an idealized array of omnidirectional isotropic point sources is shown. This assumption will be relaxed later in the presentation. The goal in radio direction finding is, given the induced complex voltages V_i at each of the antenna elements, to estimate their complex signal strengths and directions of arrival.

In adaptive processing, the objective is to extract a desired signal of interest buried in various multipaths or reflections of the signal, strong interference, and thermal noise. Generally, it is assumed that the direction of arrival of the signal is known whereas the angles of arrival of the undesired signals are not known. It is desired to extract a signal of interest (*SOI*) from the measured complex voltages V_i at the antenna elements, which are the sum of the signal of interest and other undesired signals, including noise. Always, however, in this process something about the signal is assumed to be known (1). This is the prerequisite for any adaptive system. The *a priori* information may be available in any of the following forms: (1) the direction of arrival of the signal, (2) some special temporal characteristics like cyclostationarity or constant modulus, or (3) some statistical information, such as that the desired signal and the undesired signals are statistically independent.

Stochastic Versus Direct-Data-Domain Approach

Historically, almost all algorithms in radio direction finding and adaptive processing have used algorithms that are based on stochastic methodology so that the algorithm performs in an optimum sense on the average. With the advent of the digital revolution, classical algorithms applied to analog systems are still being used in digital form. The application of a direct-data-domain method is therefore very attractive, as it allows one to obtain an optimum solution for the data on hand and not on the average for all the data sets. In addition, the application of a direct-data-domain approach is computationally very efficient, as no covariance matrix of the data is needed. In most algorithms it is assumed that the covariance matrix of the data is given; however, in reality it is only the data themselves that are available. Hence one tries to approximate the covariance matrix from the data sets. Not only is that a very computation- intensive process, but also, it is difficult to estimate the error that is incurred in this approximation. In addition, a direct-data-domain least-squares approach has a lower Cramer–Rao bound for the parameters of interest than a stochastic methodology (2).

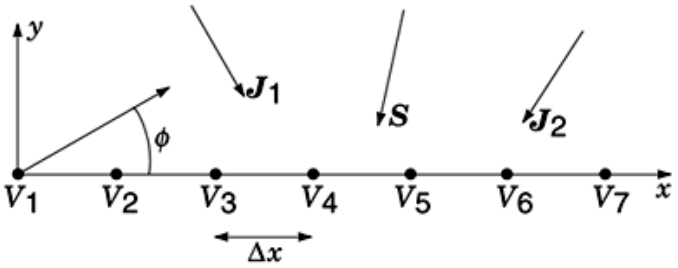

Fig. 1. An array of omnidirectional isotropic point sources.

A case is made here for applying the methodology directly to the data set at hand, which provides a direct least-squares solution based on the available data without making any assumptions of the underlying statistics (3). In this review we will introduce the computationally efficient and numerically robust direct-data-domain methodology for both radio direction finding and adaptive processing. Another ramification of this approach is that it is quite straightforward to allow for mutual coupling between the sensors collecting the data. This issue is addressed later on.

Radio Direction Finding

In radio direction finding the technique is to estimate the complex intensities of the various signals incident on the antenna elements from complex signal voltages measured at the terminals of the antenna. There are several assumptions that are involved in the processing. First, the sources of the signals are assumed to be located in the far field. Far field is defined as a distance greater than $2d^2/\lambda$, where d is the largest physical dimension of the antenna array and λ is the wavelength of the signal. The far-field assumption implies that the wavefront of the signal arriving at the array is essentially planar.

Another assumption that is generally used is that the antennas are omnidirectional point radiators so that there is no mutual coupling between the elements. However, this is a highly idealized situation. It is never true in real life, and hence, unless the electromagnetic effects (from solution of Maxwell's equations) are taken into account, use of pure signal-processing algorithms will not provide meaningful results in a real environment. First, we present the methodology for estimating the direction of arrival for idealized omnidirectional point sources. Then, the effects of mutual coupling, when using realistic antennas, can be allowed for by electromagnetic preprocessing of the data as outlined in the section on adaptive processing below.

Case A: Uniform Linear Array (Antenna Elements Are Uniformly Spaced). When the omnidirectional point-source antenna elements are uniformly spaced, the complex voltage V_n induced in an antenna element n is given by

$$V_n = \sum_{i=1}^{P} A_i \exp\left\{\frac{j2\pi d_n}{\lambda}\cos\phi_i\right\} + \text{noise} \qquad (1)$$

where d_n is the location of the nth antenna element, ϕ_i is the direction of arrival of the signal from the end-fire direction as shown in Fig. 1, and A_i is its complex amplitude. P is the total number of signals incident on the array and needs to be determined. For a uniformly spaced array $d_n = nd$, where $d = \Delta\chi$ is the interelement spacing (as per Fig. 1). Here we have used a single snapshot, i.e., the phasors V_n are measured across the entire

array at a single time instant. It is further stipulated that all P signals are narrowband and the wavelength of transmission is λ. So the goal here is to estimate the $2P$ unknowns of A_i and ϕ_i from the measured voltages V_n. As long as there are $2P$ antenna elements, the problem can be solved by fitting a sum of complex exponentials to the voltages V_n. This is computed through the matrix-pencil approach (4,5,6), which is very robust when applied to noisy data. Of course, in a real situation there is noise in the data and hence we need more than $2P$ antenna elements. The conventionally used methodology of ESPIRIT (7,8) requires the formation of a covariance matrix, which is computationally more intensive than the Matrix-Pencil Technique. From a statistical point of view both the methods have similar variances for the estimates in presence of noise. However, it is important to note that additional processing is required, as in ROOT-MUSIC, where actual directions of arrival are obtained, which involves factoring a high-order polynomial to estimate the strengths of the various signals.

Case B: Nonuniformly Spaced Elements (Antenna Elements Are Nonuniformly Spaced). When the antenna elements are spaced nonuniformly, then clearly the above approach based on a single snapshot is not applicable. The processing is to be done in the time domain. In that case one uses the model

$$V_n(t) = \sum_{i=1}^{P} A_i \exp\left(\frac{j2\pi d_n}{\lambda} \cos\phi_i\right) \exp(j2\pi f_0 t)\, \exp(j\psi_i) \qquad (2)$$

where d_n is the location of the nth antenna element, f_0 is the frequency of transmission, and ϕ_i is the phase associated with the ith incident field. Therefore, A_i is considered to be real. It is important to note in this scenario that if there are coherent multipaths (i.e., the signal and an undesired multipath component of the signal are in phase), a nonuniformly spaced array cannot separate them from a single snapshot without any additional processing. Temporal information is also necessary (9). The various components can be extracted using MUSIC (7) and many of its derivatives, and also ESPIRIT (7) may be used for a certain class of array geometries.

Adaptive Processing Using The Spatial-Domain Least-Squares Approach

In the conventional adaptive beam-forming methodology each antenna element is weighted. The processing of information is done over time as the correlation matrix $\boldsymbol{R}$ of the data needs to be formed (10). In the current development we deal with a single frame or a single snapshot. A single snapshot is defined as the set of complex voltages V_n measured at each one of the $N + 1$ antenna elements at a particular instant of time. These measured voltages V_n, $n = 0, 1, \ldots, N$, contain the desired signal plus jammer, clutter, and thermal noise components. Hence, in this development one can allow for blinking jammers, time-varying clutter, and coherent multipath components. The price one pays for dealing with a snapshot (frame) is that the number of degrees of freedom is limited to $N/2$, as opposed to $N + 1$ in the covariance-matrix-based approaches. However, this limitation is alleviated by doubling the available data, as illustrated later (11,12,13,14). In this model we double the number of data by not only considering them in the forward direction but also conjugating them and reversing the direction of increment of the independent variable; we call this the *backward method* [1]. This type of processing can be done as long as the series to be approximated can be fitted by exponential functions of purely imaginary argument. This is always true for the adaptive-array case. So by considering the data set $x(k)$ and $x*(-k)$ we have essentially doubled the amount of data without any penalty, as these two data sets for our problem are linearly independent. Next we use these data to find the adaptive weights, which are related to the directions of arrival of the jammers.

Often, due to uncertainties in the direction of arrival of the SOI, there may be signal cancellation in the adaptive process. The expected signal (target return) may not arrive from a single predetermined angle, but, due to refractions of the atmosphere, arrive over a finite angle extent. In addition, there is always a mismatch

between the look-direction constraint and the true direction of arrival of the desired signal. Correction for this uncertainty is accomplished in the least-squares procedures by establishing look-direction constraints at multiple angles of the adaptive receiver pattern within the transmitter main-beam extent. The multiple constraints are established by using a uniformly weighted array pattern for the same-size array as the adaptive array under consideration. Multiple points of constraints in the received adaptive beam pattern to be formed are chosen for the nonadapted array pattern, and a row corresponding to each constraint is implemented in the matrix equations presented below:

$$\begin{bmatrix} 1 & Z_0 & \cdots & Z_0^M \\ 1 & Z_1 & \cdots & Z_1^M \\ 1 & Z_2 & \cdots & Z_2^M \\ \vdots & \vdots & & \vdots \\ 1 & Z_L & \cdots & Z_L^M \\ X_0 - Z_0^{-1}X_1 & X_1 - Z_0^{-1}X_2 & \cdots & X_M - Z_0^{-1}X_{M+1} \\ \vdots & \vdots & & \vdots \\ X_{M-1} - Z_0^{-1}X_M & X_M - Z_0^{-1}X_{M+1} & \cdots & X_{N-1} - Z_0^{-1}X_N \\ X_N^* - Z_0^{-1}X_{N-1}^* & X_{N-1}^* - Z_0^{-1}X_{N-2}^* & \cdots & X_M^* - Z_0^{-1}X_{M-1}^* \\ \vdots & \vdots & & \vdots \\ X_{M+1}^* - Z_0^{-1}X_M^* & X_M^* - Z_0^{-1}X_{M-1}^* & \cdots & X_M^* - Z_0^{-1}X_{M-1}^* \end{bmatrix}_{(L+N-2)\times(M+1)}$$

$$\times \begin{bmatrix} W_0 \\ W_1 \\ \vdots \\ W_M \end{bmatrix}_{(M+1)\times 1} = \begin{bmatrix} C_0 \\ C_1 \\ \vdots \\ C_L \\ 0 \\ \vdots \\ 0 \end{bmatrix}_{(L+N-2)\times 1} \tag{3}$$

Here Z_i represent the various constraints along specific look directions of: the receiver beam pattern and are defined by $[Z_i = \exp(j2\tau d/\lambda)\cos\phi_i]$. Z_0 corresponds to the SOI. Here X_i are the actual voltages measured at the ith antenna element due to SOI, jammer, clutter, and thermal noise. W_i are the adaptive weights, and C_i are numerical prefixed values of the constraints imposed on the adapted beam to be formed. Let L be the number of look-direction constraints, and $M + 1$ be the number of weights to be calculated. Therefore $M - L + 1$ is the number of jammers that can be nulled.

The first $L + 1$ equations in Eq. (3) define the main beam constraints of the adapted receiver pattern. The remaining equations use data from the $N + 1$ elements, and each entry computes the difference between neighboring elements, thereby canceling the SOI and hence containing only undesired signal components. The number of equations must equal the number of weights, and therefore $M = L + N - M$. This leads to the relationship $N = 2M - L$ between the number of weights, number of constraints, and number of elements. Using the forward–backward data from a single snapshot, the maximum number of weights or the degrees of freedom that can be achieved for a direct-data-domain approach is approximately $N/1.5 + 1$, as opposed to N

+ 1 for the conventionally used statistical method. So there is a slight loss in the degrees of freedom. However, we gain the ability to deal with a highly nonstationary environment where the signal environment may change even from a snapshot to snapshot and thereby allow for blinking jammers.

In a phased array, the angle extent of the received beam is established by the main beam of the transmitted wave (usually between the 3 dB points of the transmitted field pattern). Target returns within the angle extent must be coherently processed, but with the appropriate steering vector. In that case, the excitation function Y [right-hand side of Eq. (3)] would have several nonzero elements, depending on the number of constraints used for the main beam. This is called a multiple-constraint receive beam pattern, as opposed to constraining it at a single point based on the assumed direction of arrival of the signal of interest. The advantage of dealing with multiple constraints as opposed to a single constraint in the main beam is illustrated next.

Consider a 21-element array with $N = 20$ and $M = 11$. The beam is considered to be pointed broadside ($\theta = 90^\circ$), and target returns can be expected over the main beam out to the 3 dB points ($\pm 5^\circ$). For the broadside-pointed array, consider a target located in the main beam at $\theta = 94^\circ$ instead of $\theta = 90^\circ$. The target signal-to-noise ratio at each element is 20 dB, and we assume no jammers or clutter present. Figure 2 shows the main-beam region of the antenna pattern after adaptation. Since the target is not at the look-direction constraint point (i.e., $\theta = 90^\circ$), the adaptive process considers it as an interfering source and attempts to null it. Because the target is relatively near to the look-direction constraint, the process is not able to form a perfect null. Figure 3 shows the complex array gain along the target direction for 10 random samples of the noise. The point $\times$ represents the nonadapted array gain in the target direction. Note that the gain in the target direction is reduced in each case. In addition, there is a wide variation in the array gain from one random sample to the other. Now, if one were to process the returns from different pulses in a pulse burst that was to be coherently integrated, then this variation in the received signal would have significant influence on that integration. We now illustrate how to overcome it.

We establish a multiple constraint on the receive pattern as shown in Fig. 4 at 85°, 87.5°, 90°, 92.5°, and 95°. So the receive signal would not be nulled if it were located anywhere within the 10° beam width. For this particular case, the excitation vector $\boldsymbol{Y}$ would be of the form $\boldsymbol{Y}^{\mathrm{T}} = [13,\ 7.72 + j8.32,\ 7.72 - j8.32,\ -0.816 + j7.149,\ -0.816 - j07.149,\ 0,\ 0,\ 0,\ 0,\ 0,\ 0,\ 0,\ 0]$. The corresponding receive beam pattern with the five constraints is shown in Fig. 4. We now consider the same example as before. However, as seen from Fig. 5 (using the same data from 10 random samples of noise), there is no reduction of the array gain along the direction of the target, and for all the ten runs the array gain vectors are very nearly aligned. The five-constraint approach permits effective radar processing across the main beam's extent with no effect of the loss of gain in the target direction. The adaptive process has been prevented from nulling the target.

In summary, the main-beam constraint allows the look-direction constraint to be established over a finite beam width while maintaining the ability to adaptively null jammers in the side-lobe region. Although the main-beam gain can become degraded if the signal becomes very strong, this does not appear to be a serious limitation for practical radar-processing.

Incorporation Of Mutual Coupling In Adaptive Antennas

To illustrate the importance of mutual coupling between antenna elements in a phased array, we consider signal recovery by a linear array of equispaced, thin, half-wavelength dipoles as shown in Fig. 6. However, in this analysis the antennas can be any complex composite element. The method of moments (*MOM*) is used to perform the electromagnetic analysis of the antenna array. Using a Galerkin formulation, the entries of the MOM impedance matrix measure the interaction between the basis functions, i.e., they quantize the mutual coupling (15,16). The electromagnetic analysis needs to be coupled with the signal-processing algorithms in order to generate accurate and reliable results (17,18). These ideas are explained through an array of N_{e} uniformly spaced isotropic point sensors as shown earlier in Fig. 1. The array receives a signal (called S) from a

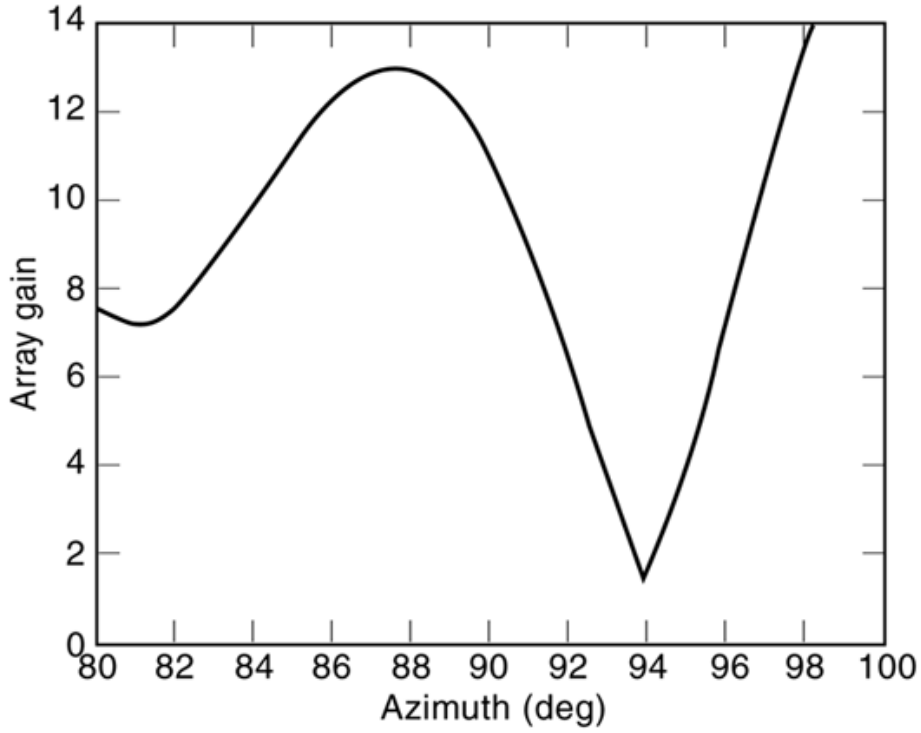

Fig. 2. Main-beam array gain with a strong target at 94°.

known direction ϕ_0 and some interference sources (called J_i) from unknown directions. In the absence of mutual coupling, each individual source presents a linear phase progression across the face of the array. Therefore, the voltage at the i-th element due to the incident fields is

$$V_i = Se^{jk(i-1)\,\Delta x\,u_0} + \sum_{m=1}^{M_e} J_m e^{jk(i-1)\,\Delta x\,u_m} + n_i, \qquad i = 1, \ldots, N_e \tag{4}$$

where, $u_m = \cos\,\phi_m$, S is the complex intensity of the signal incident from direction ϕ_0, J_m is the intensity of the mth interference source arriving from direction ϕ_m, and n_i is the additive noise at each element. Let $\beta = \exp(jk\ \Delta x\ u_0)$ represent the phase progression of the signal between one element and the next. Hence, the term $V_i - \beta^{-1}V_{i+1}$ has no signal component. This is illustrated through the last K equations of Eq. (3), where, $K = (N_e + 1)/2$.

The last $K - 1$ rows of the matrix contain only interference and noise terms. Setting the product of these terms with the weights to zero nulls the interference in a least-squares sense. The equation represented by the first few rows constrains the gain of the array along the direction of the signal. It can be shown that if $M + 1 \leq K$, the signal can be recovered and

$$S = \sum_{i=1}^{K} w_i V_i \tag{5}$$

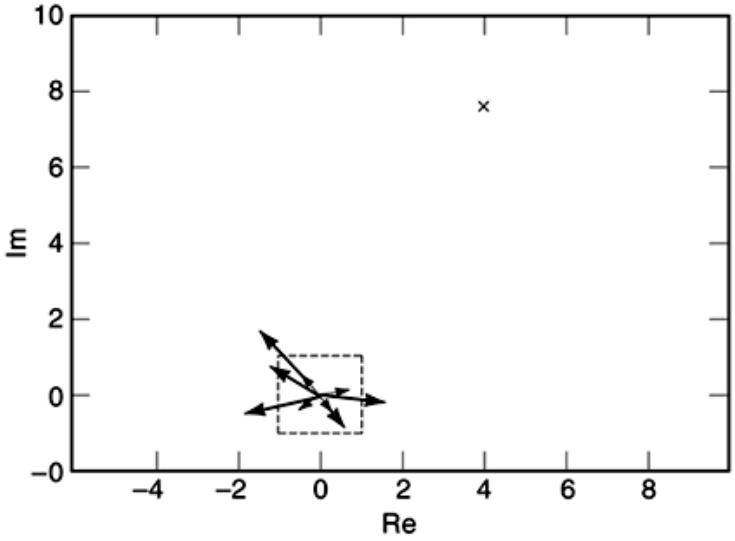

Fig. 3. Complex array gain: one constraint.

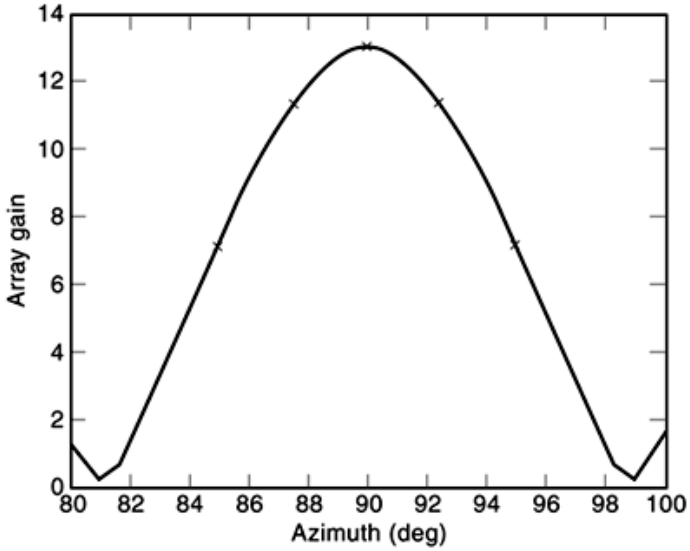

Fig. 4. Uniformly weighted array pattern with the location of the five constraints.

It is important to point out that there may be signal cancellation if the actual direction of arrival of the signal of interest is slightly different from the assumed direction of arrival. However, this can be avoided by selecting the first row of the matrix and replacing it by placing an *a priori* 3 dB constraint on the receive beam width of the adaptive pattern as the optimization process progresses. This prevents signal cancellation when there is uncertainty in the direction of arrival.

Let us consider a signal corrupted by three jammers that are incident on the array. To focus only on the effects of mutual coupling, it is first assumed that there is no mutual coupling between the antenna elements

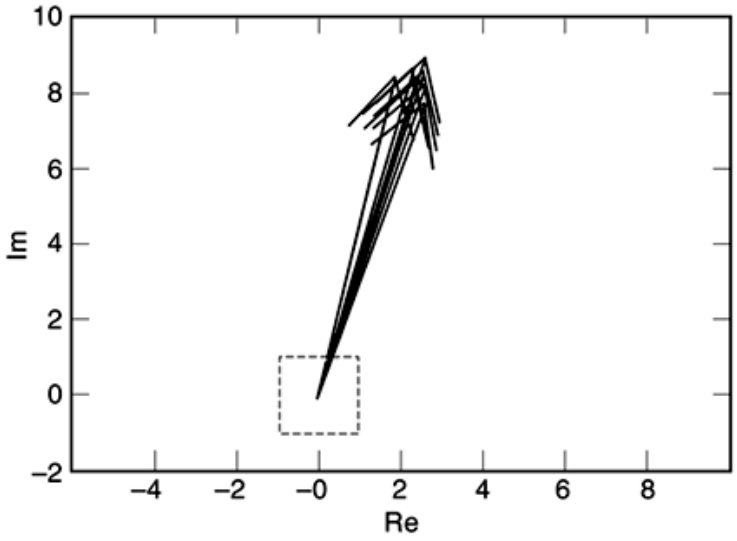

Fig. 5. Complex array gain: five constraints.

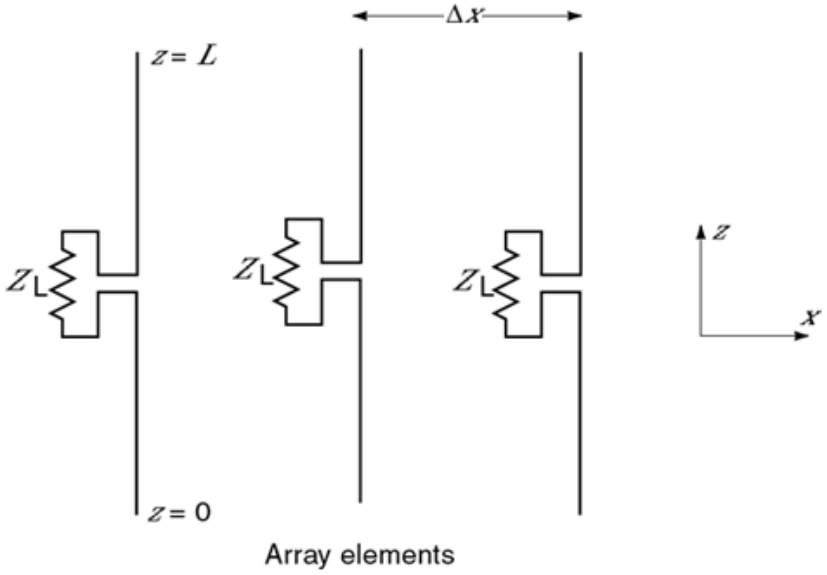

Fig. 6. A realistic adaptive antenna array.

and the voltages at the ports of the array is given by Eq. (4). These voltages are then passed to the signal recovery subroutine to find the adaptive weight using Eq. (3), and the signal is estimated using Eq. (5). Next, we consider a realistic antenna array as shown in Fig. 6, where each wire antenna element is centrally loaded with an impedance.

The details of the chosen array are presented in Table 1 and illustrated in Fig. 5. The receiving algorithm tries to maintain the gain of the array in the direction of $\phi_0 = 45^\circ$ while automatically placing nulls at in the interference directions. All signals and jammers arrive from the elevation $= 90^\circ$. The base signal and jammer

Table 1: Details of Example Array

Number of elements in array	7
Length of z-directed wires	$\lambda/2$
Radius of wires	$\lambda/200$
Spacing between wires	$\lambda/2$
Loading at the center	50 Ω

Table 2: Base Signal and Jammer Values

	Magnitude (V/m)	Phase	DOA (deg)
Signal	1.0	0.0	45
Jammer 1	1.0	0.0	75
Jammer 2	1.5	0.0	60
Jammer 3	2.0	0.0	30

intensities and directions of arrival ϕ_i are given in Table 2. In all simulations the jammer intensities, the directions of arrival of the jammers, and the signal intensity are used only to find the voltages input to the receiving algorithm. The receiving algorithm itself uses only the direction of arrival of the signal; that is, only the look direction is considered to be known.

The signal is kept constant at 1.0 V/m as given in Table 2. The intensity of the first jammer, arriving from $\phi = 75^\circ$, is varied from 1.0 V/m (0 dB with respect to the signal) to 1000.0 V/m (60 dB) in steps of 5 V/m. If the jammers are properly nulled, we expect the reconstructed signal to have no residual jammer component. Therefore, as the jammer strength is increased, we expect the reconstructed signal to remain constant.

Figure 7(a) presents the results on the magnitude, and Fig. 7(b) on the phase, for the adapted signal using the receiving algorithm when mutual coupling is absent and the antenna array is considered to be an ideal one as shown in Fig. 1. The magnitude of the reconstructed signal is indistinguishable from the expected value of 1.0 V/m. This figure demonstrates that, in the absence of mutual coupling, the receiving algorithm is highly accurate and can still null a strong jammer.

Figure 8(a,b) show the results for the magnitude and phase, respectively, of the received signal when using the measured voltages that are affected by mutual coupling. Here, the array consists of seven wires. The magnitude of the reconstructed signal varies approximately linearly with respect to the intensity of the jammer. This is because the strong jamming is not nulled and the residual jammer component completely overwhelms the signal.

The reason the signal cannot be recovered when mutual coupling is taken into account can be understood visually by comparing the adapted beam patterns in the ideal case of no mutual coupling with the case where mutual coupling is present. In Fig. 9(a) we see the beam pattern for the ideal case. The pattern clearly displays the three deep nulls at the directions of the interference. The high side lobes are in the region where there is no interference. Because of the deep nulls, the strong interference can be completely nulled and the signal recovered correctly. Figure 9(b) shows the beam pattern when the mutual coupling is taken into account. As is

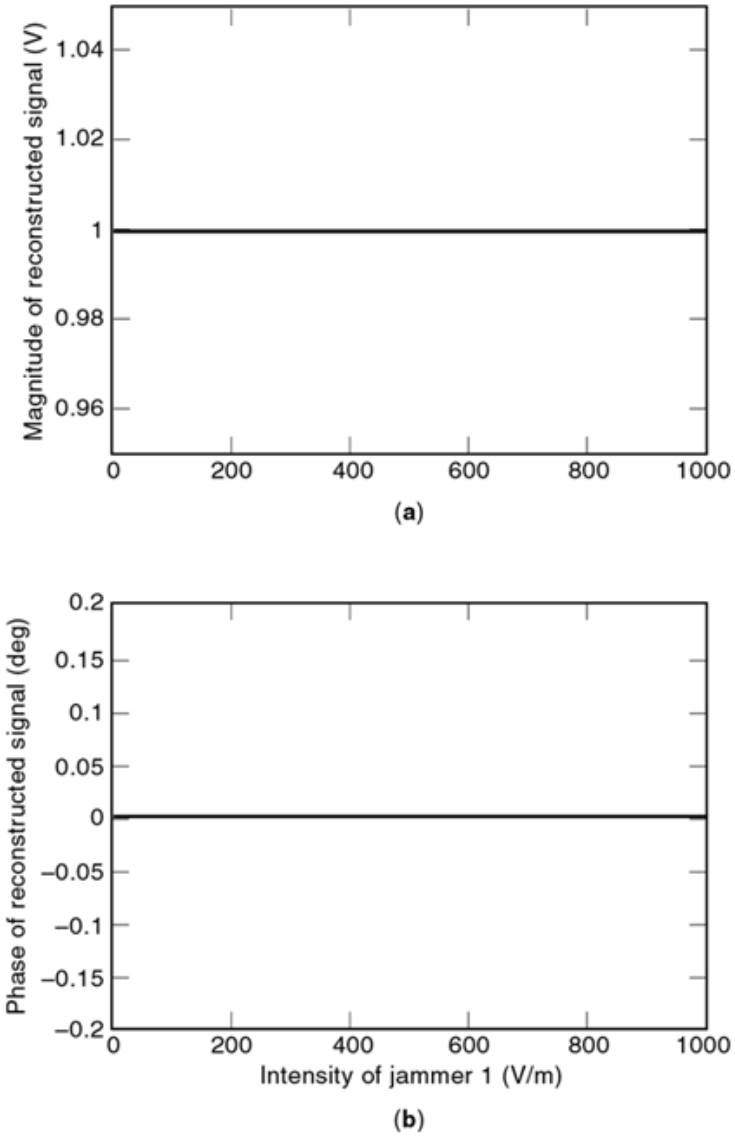

Fig. 7. Signal recovery for an idealized array without mutual coupling.

clear, the gain of the antenna along the signal direction is considerably reduced. The pattern nulls are shallow and are displaced from the desired locations. The shallow nulls result in inadequate nulling of the interference; hence the signal cannot be recovered.

The receiving antenna is next assumed to be a linear array of N_e elements as illustrated in Figure 6. The elements are parallel, thin equispaced dipoles. Each element of the array is identically point loaded at the center. The dipoles are x-directed, of length L and radius a, and are placed along the x axis, separated by distance Δx. The array lies in the X–Z plane.

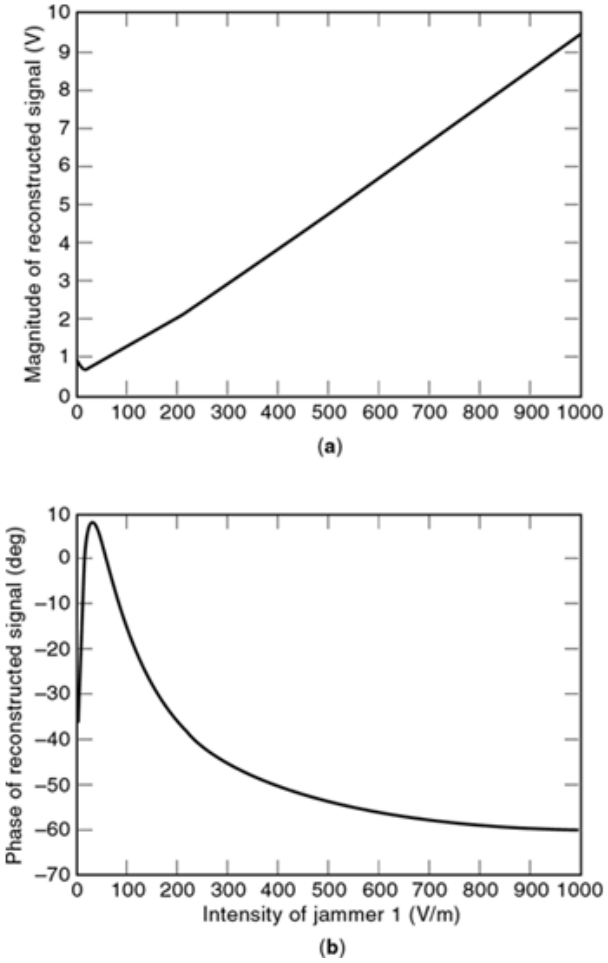

Fig. 8. Signal recovery for a realistic array in the presence of mutual coupling.

We begin by analyzing the response of the antenna array to an incident field E^{inc}. Since the array is composed of thin wires, the following simplifying assumptions are valid (15,16): (1) The current flows only in the direction of the wire axes (here the z direction). (2) The current and charge densities on the wire are approximated by filaments of current and charge on the wire axes (which lie in the $y = 0$ plane). (3) Surface boundary conditions can be applied to the relevant axial component of the wire axes.

The integral equation that characterizes the current on the wires and describes the behavior of the array is (15,16)

$$E_z^{\text{inc}} = -\mu_0 \int_{\text{axes}} I(z') \frac{e^{-jkR}}{4\pi R}\, dz' + \frac{1}{\varepsilon_0} \frac{\partial}{\partial z} \int_{\text{axes}} \frac{\partial I(z')}{\partial z'} \frac{e^{-jkR}}{4\pi R}\, dz' \qquad (6)$$

We solve this equation using the method of moments to obtain the MOM impedance matrix. The basis functions used are piecewise sinusoids as described in Ref. 15 and shown in Fig. 10. P (chosen odd) basis functions are used per element. Using these basis functions and a Galerkin formulation, Eq. (6) is reduced to

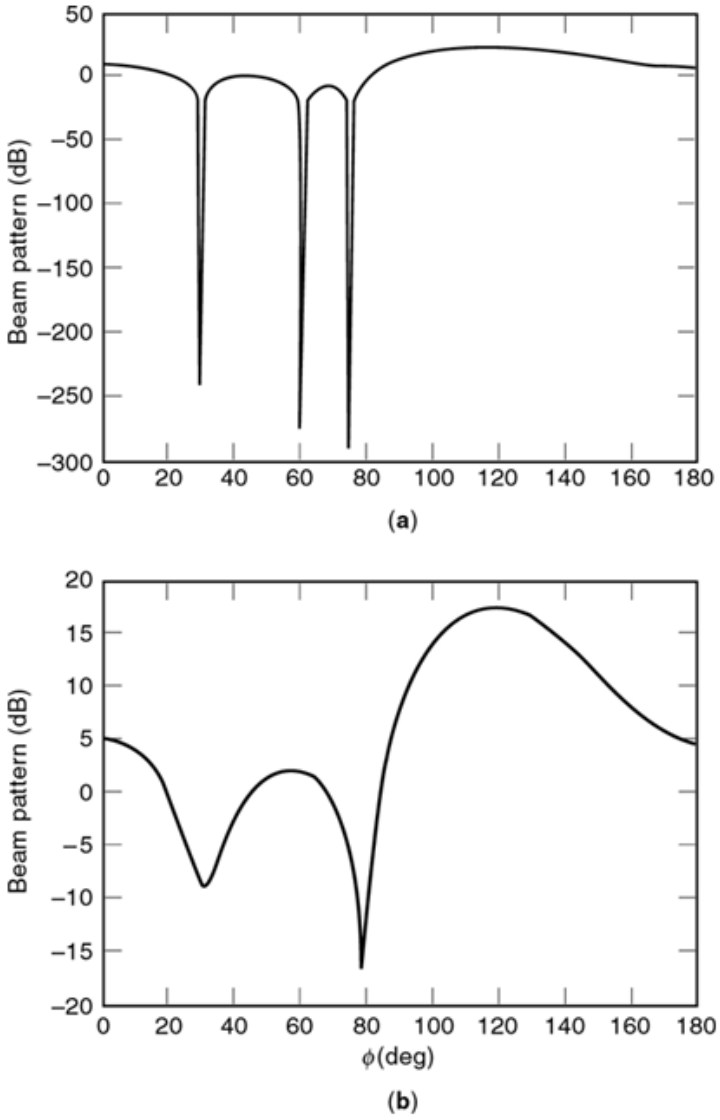

Fig. 9. Antenna beam pattern, (a) for an idealized array without taking into account mutual coupling in the analysis, and (b) for a realistic array.

the matrix equation

$$\boldsymbol{V} = \boldsymbol{Z}\boldsymbol{I} \Rightarrow \boldsymbol{I} = \boldsymbol{Y}\boldsymbol{V} \tag{7}$$

where $\boldsymbol{I}$ is the MOM current vector containing the coefficients of the expansion of the current in the sinusoidal basis, $\boldsymbol{V}$ is the MOM voltage vector representing the inner product of the weighting functions and the incident field, and $\boldsymbol{Z}$ and $\boldsymbol{Y}$ are the MOM impedance and admittance matrices respectively. Both matrices are of order $N \times N$, where $N = N_e P$ is the total number of unknowns used in the MOM formulation.

Assuming that the incident field is linearly polarized and arrives from direction (θ, ϕ), it can be written in the functional form as

$$E_z^{\text{inc}} = E_0\, e^{-j\boldsymbol{k}\cdot\boldsymbol{r}} \tag{8}$$

where $\boldsymbol{k} = -k(\hat{a}_x \cos\phi \sin\theta + \hat{a}_y \sin\phi \sin\theta + \hat{a}_z \cos\phi)$ is the wave vector associated with the direction of arrival of the incident signal. Using P(odd) basis functions on each antenna, the current on the structure can be written as

$$I(z) = \sum_{n=1}^{N_w} \sum_{p=1}^{P} I_{p,n} f_{p,n}(z)$$

where $f_{p,n}(z)$ is the p-th basis function on the nth element whose functional form is given by

$$f_{p,n}(z) = \begin{cases} \dfrac{\sin[k(z - z_{p-1,n})]}{\sin k\Delta z} & z_{p-1,n} \le z < z_{p,n} \\ \dfrac{\sin[k(z_{p+1,n} - z)]}{\sin k\Delta z} & z_{p,n} \le z < z_{p+1,n} \\ 0 \qquad \text{otherwise} \end{cases} \tag{9}$$

where $\Delta z = L/(P+1)$ and $z_{p,n} = z_{0,n} + p\Delta z$. $z_{0,n}$ is the z-coordinate of the bottom of the n-th antenna as shown in Fig. 10. Substituting Eq. (9) in (6) and using testing functions $f_{q,m}(z)$, the entries of $[V]$ are given by

$$V_i = \frac{E_0\, e^{jkx_m \cos\phi \sin\theta}}{k \sin(k\Delta z) \sin^2\theta} 2e^{jkz_{q,m}\cos\theta} \left[\cos(k\Delta z \cos\theta) - \cos(k\Delta z)\right]$$

where x_m is the x-coordinate of the axis of the m-th antenna. For the impedance matrix $[Z]$ the elements are given by

$$Z_{i,\ell} = \frac{j30}{\sin^2(k\Delta z)} \int_{z_{q-1,m}}^{z_{q,m}} \sin[k(z - z_{q-1,m})] \left\{ \frac{e^{-jkR_1}}{R_1} - 2\cos(k\Delta z) \frac{e^{-jkR_2}}{R_2} + \frac{e^{-jkR_3}}{R_3} \right\} dz$$

$$+ \frac{j30}{\sin^2(k\Delta z)} \int_{z_{a,m}}^{z_{q+1,m}} \sin[k(z_{q+1,m} - z)] \left\{ \frac{e^{-jkR_1}}{R_1} - 2\cos(k\Delta z) \frac{e^{-jkR_2}}{R_2} + \frac{e^{-jkR_3}}{R_3} \right\} dz$$

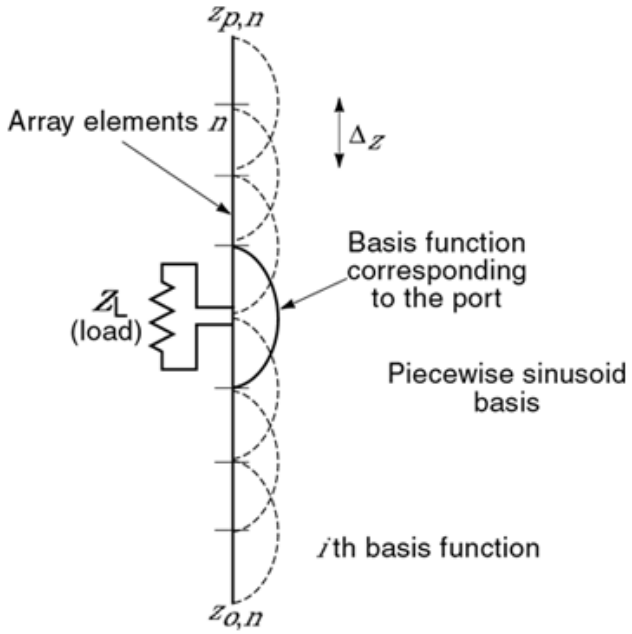

Fig. 10. Basis functions assumed in the electromagnetic analysis using the MOM analysis.

with

$$R_1 = \sqrt{(x_m - x_n)^2 + (z - z_{p-1,m})^2}$$

$$R_2 = \sqrt{(x_m - x_n)^2 + (z - z_{p,n})^2}$$

$$R_3 = \sqrt{(x_m - x_n)^2 + (z - z_{p+1,n})^2}$$

For the case $m = n$, i.e., both subsections i and l are on the same antenna element, the term $(x_m - \mathrm{x}_n)$ is set to a, the radius of the wire (15). An analytic expression for the entries of the MOM impedance matrix is derived in Ref. 15.

Because of the choice of a piecewise sinusoid basis and the choice of an odd number of basis functions per antenna element, only one basis function is nonzero at the port. This is illustrated in Fig. 10, where the basis function $\boldsymbol{Z}_{\mathrm{L}}$ is the only one contributing to the current at the port. Therefore, the measured voltage at the port of the nth antenna is given by

$$V_{\mathrm{meas},m} = Z_{\mathrm{L}} I_{P+1/2,m} \tag{10}$$

i.e., the measured voltage at a port of the array is directly proportional to the coefficient of the basis function corresponding to the port. The MOM analysis results in a matrix equation that relates the coefficients of the current expansion to the MOM voltages through the admittance matrix. Since the MOM impedance and admittance matrices are independent of the incident fields, they can be evaluated *a priori*. The measured

voltages at the ports of the antenna are related to the current coefficients by Eq. (10). Using this equation and Eq. (7), the N_e-dimensional vector of measured voltages can be written as

$$\boldsymbol{V}_{\text{meas}} = \boldsymbol{Z}_{\text{L}} \boldsymbol{Y}_{\text{port}} \boldsymbol{V} \tag{11}$$

where $\boldsymbol{Z}_{\text{L}}$ is the $N_e \times N_e$ diagonal matrix with the load impedances as its entries, $\boldsymbol{Y}_{\text{port}}$ is the matrix with the rows of $\boldsymbol{Y}$ that correspond to the ports of the array, [$\boldsymbol{V}$] is the MOM voltage vector of order N, i.e., the number of unknowns in the MOM analysis, and $\boldsymbol{Y}_{\text{port}}$ is a rectangular matrix of order $N_e \times N$ with $N > N_e$. Since $\boldsymbol{Y}_{\text{port}}$ is a rectangular matrix with more columns than rows, Eq. (9) represents an underdetermined system of equations. Our goal is to estimate some part of $\boldsymbol{V}$ given V_{meas}. Therefore, we need a method to collapse the $N_e \times N$ matrix $\boldsymbol{Y}_{\text{port}}$ to an $\boldsymbol{N}_e \times \boldsymbol{N}_e$ matrix.

The proposed method is most easily understood when illustrated with an example. If P unknowns are used per wire element, $N = N_e P$. Consider the case with $N_e = 2$ and $P = 3$. Then $N = 6$, and basis function 2 corresponds to the port on the first element, while basis function 5 corresponds, to the port on the second element. In this case, Eq. (11) can be written as

$$\begin{bmatrix} V_{\text{meas1}} \\ V_{\text{meas2}} \end{bmatrix} = \begin{bmatrix} Z_{\text{L}} & 0 \\ 0 & Z_{\text{L}} \end{bmatrix} \begin{bmatrix} Y_{21} & Y_{22} & Y_{23} & Y_{24} & Y_{25} & Y_{26} \\ Y_{51} & Y_{52} & Y_{53} & Y_{54} & Y_{55} & Y_{56} \end{bmatrix} \begin{bmatrix} V_1 \\ V_2 \\ V_3 \\ V_4 \\ V_5 \\ V_6 \end{bmatrix} \tag{12}$$

If the signal and all the jammers are incident from approximately the same elevation θ, the entries in $\boldsymbol{V}$ are not all independent of each other. From Eq. (7), if weighting functions i and $i + 1$ belong to the same array element,

$$V_{i+1} = \left(e^{jk\,\Delta z\,\cos\theta}\right) V_i \tag{13}$$

Letting $\alpha = e^{jk\Delta z \cos\theta}$, we have

$$V_1 = e^{-jk\,\Delta z\,\cos\,\theta}\, V_2 = \alpha^{-1} V_2 \tag{14}$$

$$V_3 = e^{jk\,\Delta z\,\cos\,\theta}\, V_2 = \alpha V_2 \tag{15}$$

$$V_4 = e^{-jk\,\Delta z\,\cos\,\theta}\, V_5 = \alpha^{-1} V_5 \tag{16}$$

$$V_6 = e^{jk\,\Delta z\,\cos\,\theta}\, V_5 = \alpha V_5 \tag{17}$$

Therefore, Eq. (12) can be reduced to

$$\begin{bmatrix} V_{\text{meas1}} \\ V_{\text{meas2}} \end{bmatrix} = \begin{bmatrix} Z_{\text{L}} & 0 \\ 0 & Z_{\text{L}} \end{bmatrix} \begin{bmatrix} \alpha^{-1}Y_{21} + Y_{22} + \alpha^{-1}Y_{23} & \alpha^{-1}Y_{24} + Y_{25} + \alpha Y_{26} \\ \alpha^{-1}Y_{51} + Y_{52} + \alpha^{-1}Y_{53} & \alpha^{-1}Y_{54} + Y_{55} + \alpha Y_{56} \end{bmatrix} \begin{bmatrix} V_2 \\ V_5 \end{bmatrix}$$

$$\Rightarrow \quad \boldsymbol{V}^{\text{meas}} = \boldsymbol{B}\,\boldsymbol{V}' \tag{18}$$

where $\boldsymbol{V}'$ is the vector of length N_{e} whose entries are the MOM voltages that correspond to the ports, and $\boldsymbol{B}$ is the $N_{\text{e}} \times N_{\text{e}}$ matrix that relates the measured voltages to $\boldsymbol{V}'$.

Equation (18) is a relation between the measured voltages and the MOM voltages that correspond to the ports of the array. In a practical application, the measured voltages are the given quantities and are affected by mutual coupling. The MOM voltages on the right-hand side of Eq. (18) are the voltages that are directly related to the incident fields and so are free from the effects of mutual coupling. Both vectors are of order N_{e}, the number of ports. Therefore, this equation can easily be solved for the MOM voltages corresponding to the ports of the antenna. Furthermore, if the elevation angle of interest (θ) is fixed, the matrix $\boldsymbol{B}$ can be evaluated *a priori*. Hence the computational cost of eliminating the mutual coupling is limited to the solution of a small matrix equation.

The open-circuit voltages are the voltages that would be measured at the ports of the array if the ports were open-circuited. In Ref. 17 the authors assume that these voltages are free of the effects of mutual coupling. However, the open-circuit voltage at a particular element is the voltage measured in the presence of the other open-circuited elements. Therefore the effect of mutual coupling has been reduced but not eliminated. Mutual coupling can be assumed to have been eliminated only when there is nothing impeding the path of the incident fields—not even the array itself.

We proceed with the same example presented earlier, where the intensity of the incident signal is held constant at 1.0 V/m. The intensity of the first jammer is varied from 1.0 V/m to 1000 V/m (60 dB above the signal) in steps of 5 V/m. For each value of the jammer intensity, the MOM voltage vector is calculated and the measured voltages are calculated. In the first scenario the measured voltages are used to find the open-circuit voltages. The open-circuit voltages are passed to the direct-data-domain algorithm of Ref. 18. In the second scenario Eq. (17) is used to find the voltage vector $\boldsymbol{V}'$. These voltages are used to recover the signal and null the jammers using the same algorithm. If the jammers are properly nulled, the reconstructed signal magnitude should remain constant as a function of jammer strength.

Figure 11 presents the results when the open-circuit voltages are used to recover the signal. As can be seen, the recovered signal shows a near-linear relation to jammer strength. This indicates that the jammer has not been adequately nulled and the residual jammer strength has overwhelmed the signal.

The results of compensating for the mutual coupling using the technique presented in this paper are shown in Fig. 12(a) for the magnitude and 12(b) for the phase. The magnitude of the reconstructed signal varies between 0.996 V/m and 1.004 V/m, that is, the error in the signal recovery is very small. This figure shows that the strong jammer has been effectively nulled and the signal can be reconstructed.

The reason that the use of the open-circuit voltages is inadequate to compensate for the mutual coupling, while the technique presented here is adequate, is illustrated using the adapted beam patterns for the two cases. The adapted beam pattern associated with using the open-circuit voltages is shown in Fig. 13(a). The nulls are placed in the correct locations. However, they are shallow, resulting in inadequate nulling of the interference.

The beam pattern associated with compensating for the mutual coupling using the technique presented in this paper is shown in Fig. 13(b). The nulls are deep and placed in the correct directions. This demonstrates that the mutual coupling has been suppressed enough to null even a strong jammer.

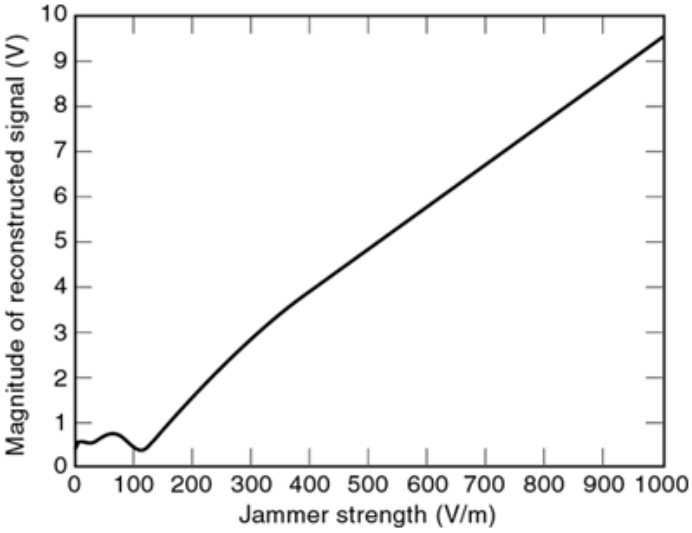

Fig. 11. Signal recovery using the open-circuit voltages.

Figures 11 and 13 allow us to conclude that using the open-circuit voltages does reduce the effect of mutual coupling somewhat. However, the reduction is inadequate to suppress strong interference. This is because the open-circuit voltage at an array element is the voltage in the presence of the other open-circuited elements. The direct-data-domain technique along with the MOM presented proves to be far superior in compensating for mutual coupling. This is because by using multiple basis functions per antenna element, the mutual-coupling information has been represented accurately.

Effect Of Noise

To illustrate the effect of thermal noise on the adaptive signal corrupted by three jammers as given in Table 3, we consider an array of z-directed dipoles that is centrally terminated by a 50 Ω resistance. Seven unknowns per wire are used in the MOM analysis, leading to a total of 91 unknowns. The signal-to-noise ratio was set at 13 dB. Note that jammer 1 is a strong jammer (66 dB with respect to the signal). For each of the 13 antenna channels, a complex Gaussian random variable is added to the measured voltages due to the signal and jammers. This set of voltages, affected by noise, is passed to the signal recovery routine described earlier. The computational procedure is repeated 500 times with different noise samples. These 500 samples are used to evaluate the mean and the variance of the parameter of interest. The output signal to interference plus noise ratio (SINR) in decibels is defined as

$$\mathrm{SINR}_{\mathrm{out}} = 10.0 \log\left(\frac{|S|^2}{|\mathrm{bias}|^2 + \mathrm{var}}\right) \tag{19}$$

The results of the above simulation are presented in Table 4. When the measured voltages are used directly to recover the signal, then—mainly due to the high bias in the estimate of the signal—the output SINR is only 6.35526 dB. The high bias can be directly attributed to the inadequate nulling of the strong jammer.

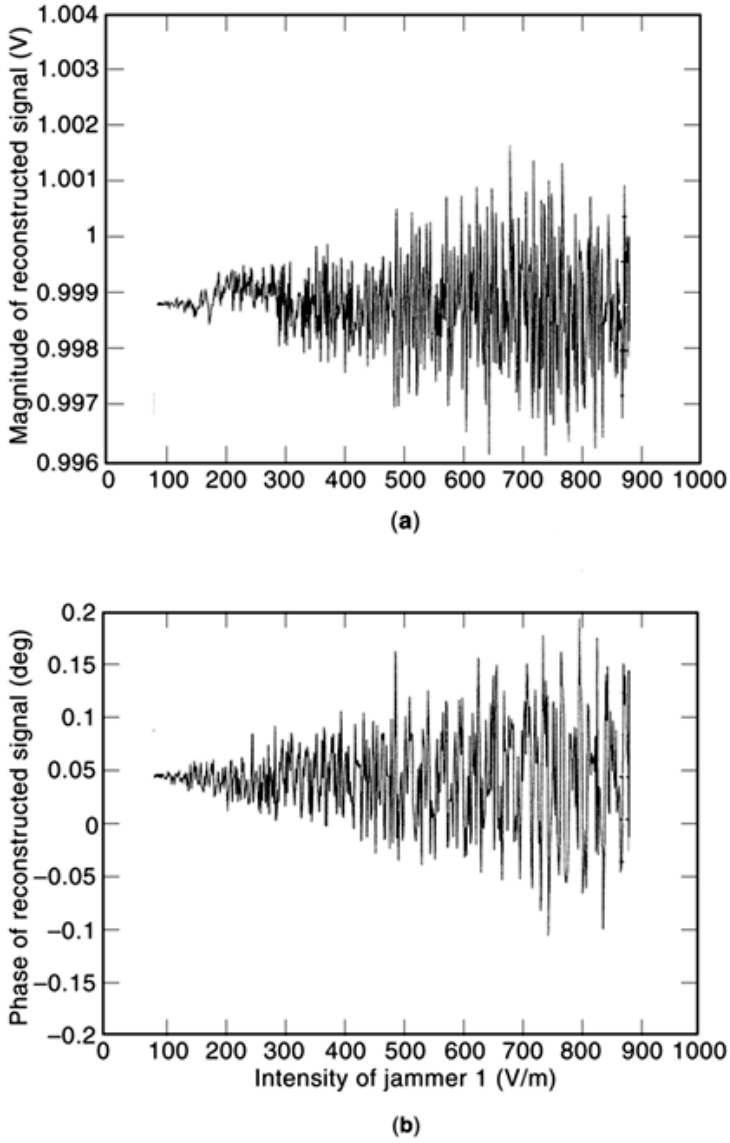

Fig. 12. Signal recovery in a realistic array after taking mutual coupling into account: (a) magnitude, (b) phase.

However, when the mutual coupling is eliminated using the technique presented in this paper, the jammers are completely nulled, yielding accurate estimates of the signal. The total interference power is suppressed to nearly 20 dB below the signal.

The examples presented here illustrate how one can effectively deal with the effects of mutual coupling between the sensors. Using the MOM with multiple basis functions per element allows us to reduce the mutual coupling to an extent where it becomes inconsequential. Hence, the effects of mutual coupling in the analysis have not been eliminated but rather taken into account.

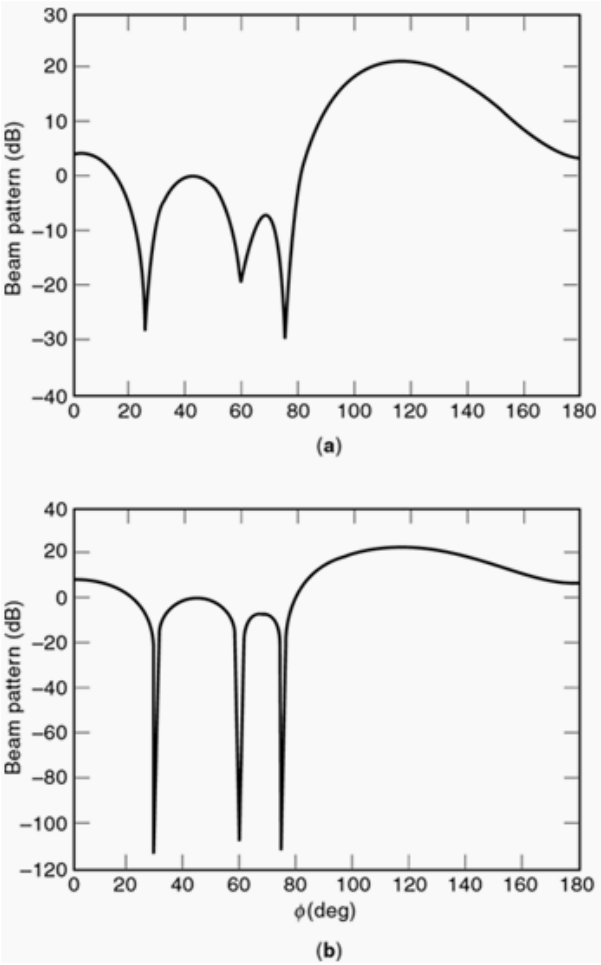

Fig. 13. Antenna beam pattern (a) using open-circuit voltages and (b) after allowing for the presence of mutual coupling.

Epilogue

For the deployment of any realistic phased arrays, the electromagnetic nature of the array must be taken into account. We have shown that the mutual coupling between the elements of the array causes adaptive algorithms to fail. This problem is associated with both covariance-matrix approaches (as stated earlier in Ref. 17) and the direct-data-domain approach (investigated here).

To properly characterize the antenna, the MOM is used. The use of multiple basis functions per element in a practical manner is a major advance and provides a pragmatic approach to the design of phased-array antennas. Recognizing that the MOM voltage vector is free from mutual coupling eliminates the mutual coupling from consideration. By using a relationship between the entries of the MOM voltage vector, a square-matrix equation is developed between the given measured voltages and the relevant entries of the MOM voltage vector. It is shown that this method works very well in the presence of strong interfering sources.

Table 3: Parameters for the Signal and Jammer

	Magnitude (V/m)	Phase	DOA (deg)
Signal	1.0	0.0	85
Jammer 1	2000.0	0.0	135
Jammer 2	1.5	0.0	60
Jammer 3	2.0	0.0	100

Table 4: Results of 500 Simulations

	Without Compensating for Mutual Coupling	After Compensating for Mutual Coupling
Input signal-to-noise Ratio	13 dB	13 dB
Number of samples	500	500
True value	(1.0, 0.0) V/m	(1.0, 0.0) V/m
Mean of 1000 estimates	(0.93337, 0.49295) V/m	(1.00379, −0.00298) V/m
Bias of estimate	(−0.06663, 0.40295) V/m	(0.00379, −0.00298)V/m
Variance of estimates	0.010448	0.0103797
Output SINR	6.35526 dB	19.86559 dB

Through a successful coupling of the electromagnetic analysis with the signal-processing algorithms used in radio direction finding and adaptive antennas, it is possible to make wide use of realistic phased-array antennas.

BIBLIOGRAPHY

1. T. K. Sarkar *et al.* A pragmatic approach to adaptive antennas, *IEEE Antennas Propag. Mag.*, **42** (2): 39–55, 2000.
2. Y. Hua T. K. Sarkar A note on the Cramer–Rao bound for 2-D direction finding based on 2-D array, *IEEE Trans. Signal Process.* **39**: 1215–1218, 1991.
3. S. Choi D. Shim T. K. Sarkar A comparison of tracking-beam arrays and switching-beam arrays operating in a CDMA mobile communication channel, *IEEE Antennas Propag. Mag.*, **41** (6): 10–22, 1999.
4. Y. Hua T. K. Sarkar Matrix pencil method for estimating parameters of exponentially damped/undamped sinusoids in noise, *IEEE Trans. Acoust. Speech Signal Process.*, **38**: 814–824, 1990.
5. T. K. Sarkar O. Pererira Using the matrix pencil method to estimate the parameters of a sum of complex exponentials, *IEEE Antennas Propag. Mag.*, **37** (1): 48–55, 1995.
6. F. Del Rio T. K. Sarkar Comparison between the matrix pencil method and the Fourier transform technique for high resolution spectral estimation, *Digital Signal Process. Rev. J.* **6** (2): 108–125, 1996.
7. P. Stoica R. Moses *Introduction to Spectral Analysis*, Englewood Cliffs, NJ: Prentice-Hall, 1997.

8. A. Medouri *et al.* Estimating one- and two-dimensional direction of arrival in an incoherent/coherent source environment, *IEICE Trans. Commun.*, **E80-B** (11): 1728–1740,1997.
9. T. K. Sarkar S. Nagaraja M. C. Wicks A deterministic direct data domain approach to signal estimation utilizing uniform 2D arrays, *Digital Signal Process. Rev. J.*, **8** (2): 114–125, 1998.
10. R. A. Monzingo T. W. Miller *Introduction to Adaptive Arrays*, New York: Wiley, 1980.
11. T. K. Sarkar N. Sangruji An adaptive nulling system for a narrow-band signal with a look-direction constraint utilizing the conjugate gradient method, *IEEE Trans. Antennas Propag.*, **37**: 940–944, 1989.
12. T. K. Sarkar *et al.* A deterministic least squares approach to adaptive antennas, *Digital Signal Process. Rev. J.*, **6** (3): 185–194, 1996.
13. S. Park T. K. Sarkar Prevention of signal cancellation in adaptive nulling problem, *Digital Signal Process. Rev. J.*, **8** (2): 95–102, 1998.
14. S. Park T. K. Sarkar A deterministic eigenvalue approach to space time adaptive processing, *Proc. IEEE Antennas and Propagation Soc. Int. Symp.*, 1996, pp. 1168–1171.
15. T. K. Sarkar B. J. Strait D. C. Kuo Special programs for analysis of radiation by wire antennas, Technical Report AFCRL-TR-73-0399, Syracuse University, June 1973.
16. A. R. Djordjevic et. al. *Analysis of Wire Antennas and Scatterers: Software and User's Manual*, Norwood MA: Artech House, 1995.
17. I. J. Gupta A. A. Ksienski Effect of mutual coupling on the performance of adaptive arrays, *IEEE Trans. Antennas Propag.*, **31**: 785–791, 1983.
18. R. S. Adve T. K. Sarkar Estimation of the effects of mutual coupling in an adaptive nulling system with a look direction constraint, *IEEE Trans. Antennas Propag.*, **48**: 2000.
19. T. K. Sarkar B. J. Strait Optimization methods for arbitrarily oriented arrays of antennas in any environment, *Radio Sci.*, **11** (12): 959–967, 1976.

TAPAN K. SARKAR
RAVIRAJ ADVE
University of Toronto
MAGDALENA SALAZAR PALMA
Polytechnic University of Madrid